Title: Laser Powder Bed Fusion for Metal Additive Manufacturing: Perspectives on Recent Developments

Authors: S.L. Sing & W.Y. Yeong*

Singapore Centre for 3D Printing, School of Mechanical & Aerospace Engineering, Nanyang Technological University

**Corresponding Author*

Designation:

Associate Professor, School of Mechanical and Aerospace Engineering, Nanyang Technological University, Singapore

Associate Chair (Students), School of Mechanical and Aerospace Engineering, Nanyang Technological University, Singapore

Programme Director (Aerospace and Defence), Singapore Centre for 3D Printing, Nanyang Technological University, Singapore

Deputy Director (Technical), HP-NTU Digital Manufacturing Corporate Lab, Nanyang Technological University, Singapore

Co-Director, NTU Institute for Health Technologies, Nanyang Technological University, Singapore

Email: wyyeong@ntu.edu.sg

Tel: (+65) 6790 5130

Abstract
While significant progress has been made in laser powder bed fusion (L-PBF) for metal additive manufacturing (AM), there is still limited large scale adoption of this advanced manufacturing technique by the industry. This paper covers the recent developments in L-PBF with discussions from the materials and process perspectives. High entropy alloys and high strength aluminum alloys have been identified as key materials development for L-PBF. Then, scanning strategies and multi-lasers applications for the process are also discussed. Other research trends and topics such as powder recycling, shape memory alloys and magnetic alloys are illustrated. The final part of this paper provides an outlook on the recent advancements while suggesting potential research topics for L-PBF.

Keywords: Additive manufacturing; 3D Printing; Powder bed fusion; Selective laser melting; Aluminum alloys; High entropy alloys; Remelting; Multi-lasers

1. Introduction

Additive manufacturing (AM) has gained much traction over the past few decades and has attracted huge attention from the industry and academia. AM has several advantages such as reducing waste materials, shorter manufacturing lead time, high flexibility, feasibility for complex geometry products and shorter product development cycle. The demand for highly customized parts, together with the change in business models and leaner suppler chains have driven the interest for AM (Gisario et al. 2019). While AM has also been used for polymers (Goh et al. 2020; Dikshit et al. 2017; Dikshit et al. 2018) and ceramics (Sing et al. 2017; Galante, Figueiredo-Pina, and Serro 2019), metal AM is still the most prominent group of techniques in terms of recent development. AM techniques are categorized into seven groups (Lee et al. 2018) and metal AM involves techniques from six of these categories and details have been reviewed

elsewhere (Gisario et al. 2019; Tan, Sing, and Yeong 2020; Buchanan and Gardner 2019). They are sheet lamination (Olivier et al. 2017), binder jetting (Lores et al. 2019), material jetting (Simonelli et al. 2019), material extrusion (Blindheim, Welo, and Steinert 2019), directed energy deposition (Eisenbarth, Soffel, and Wegener 2019) and powder bed fusion (Chahal and Taylor 2020; Tan et al. 2015).

Among all the techniques, laser powder bed fusion (L-PBF), also commonly known as selective laser melting (SLM) or direct metal laser melting (DMLM), facilitates near net shape manufacturing with one of the highest accuracies. Ample literatures that focused on L-PBF of metals or alloys are available (DebRoy et al. 2018; Gu et al. 2013; Olakanmi, Cochrane, and Dalgarno 2015; Sercombe and Li 2016; Sun et al. 2018; Wang, Wu, et al. 2019). In this perspective article, the recent developments in L-PBF are highlighted. An introduction to L-PBF is briefly provided to give an overview of the technique. The recent advances in two research areas, namely the L-PBF process and new materials for L-PBF, are discussed. The potential topics for future research in these areas are also outlined.

2. Laser Powder Bed Fusion

The L-PBF process starts from preparation of computer aided design (CAD) files which are subsequently sliced into two-dimensional (2D) layers by computer software. The layer thickness of these slices is considered as one of the process parameters. The L-PBF process includes powder deposition onto a substrate plate or previous processed layers, selectively melting of the powder particles with a high energy laser beam according to each sliced profile, lowering the platform by predetermined layer thickness and then recoating a new layer of powder. The cycle repeats till the process ends with the melting of the last sliced layer of the components (Bogue

2011). Figure 1 illustrates the schematic of L-PBF. The white fonts indicate the machine parts and the black ones are key controllable process parameters.

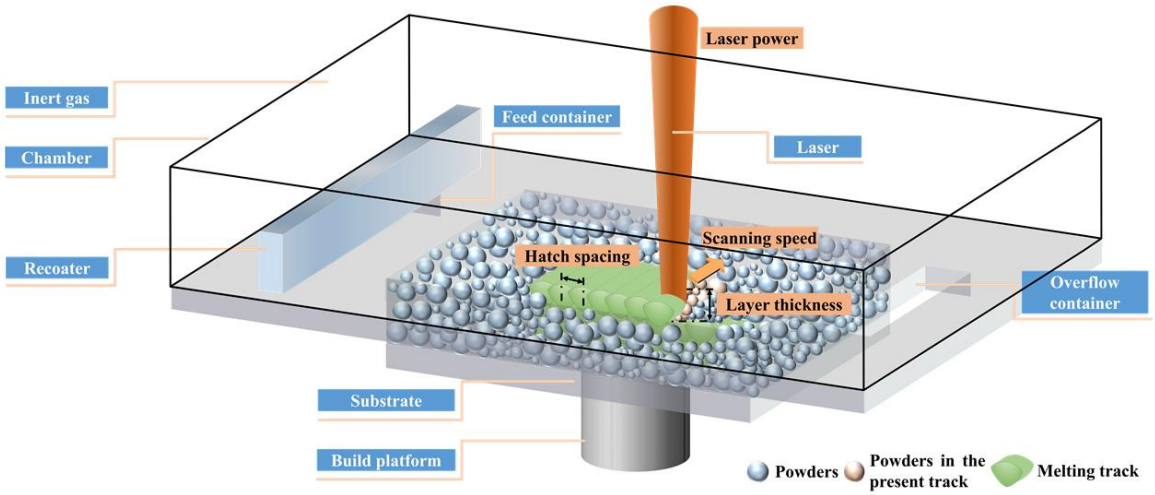

Figure 1 Schematic of L-PBF build chamber and process. The white fonts illustrate the machine components while the black fonts illustrate the key processing parameters (Yu, Sing, Chua, Kuo, et al. 2019).

L-PBF allows quick production of three-dimensional (3D) parts with complicated shapes directly from powders without the mold design process which can be time and cost extensive (Concli and Giliolo 2019). It results in superior property in parts compared to counterparts produced by conventional methods due to the ultrafine and graded microstructure attributed to the rapid cooling and solidification cycles (with cooling rate of 10^3-10^6 $^oC/s$) during the process (Yang et al. 2016; Liu et al. 2014; Yang et al. 2018).

3. Recent Materials Development for Laser Powder Bed Fusion

There has been extensive work done on material development for L-PBF and the widely known materials for L-PBF are stainless steel, tool steel, Ti6Al4V and AlSi10Mg (Yap et al. 2015). The research for these materials is well established. Recently, there have also been developments for magnesium alloys (Shuai, He, et al. 2018; Shuai et al. 2019), tungsten (Guo et

al. 2019; Wen et al. 2019), zinc alloys (Shuai, Xue, et al. 2018) and metal matrix composites (Du et al. 2020; Yu, Sing, Chua, Kuo, et al. 2019). To further expand the available materials, *in-situ* alloying has been proven to be a viable approach (Martinez, Todd, and Mumtaz 2019; Wang, Tan, et al. 2019; Wang, Liu, et al. 2019; Huang et al. 2020). In the following sections, the recent key material advancements for L-PBF are discussed.

3.1 Modified High Strength Aluminum Alloys

Among commercial aluminum alloys, mainly near eutectic AlSi alloys, such as AlSi10Mg, Al12Si are often used in L-PBF. The success of these alloys is due to the silicon content which hinders the solidification cracking, which is related to the solidification range of the alloy, fluidity of the melt and coefficient of thermal expansion. Solidification cracking has restricted the printability of most high strength aluminum alloys such as 2000, 6000 and 7000 series. Simulations have been done to understand the L-PBF of such alloys (Loh et al. 2015). In addition, these aluminum alloys contain volatile elements such as zinc, magnesium and lithium that can easily evaporate during L-PBF. To overcome these obstacles, many efforts have been made using modified aluminum alloys for L-PBF.

Kuo *et al.* studied the microstructure and mechanical properties of AlMgSc alloy (Scalmalloy) (Kuo et al. 2020). Scandium addition in aluminum alloys results in the precipitation of Al_3Sc phase which limit columnar grains formation and hot tearing. Similar observations were made by Bi *et al.* using AlMgSiScZr (Bi, Lei, Chen, Chen, Tian, Liang, et al. 2020; Bi, Lei, Chen, Chen, Tian, Qin, et al. 2020). The precipitation of secondary phases such as Al_3Sc, Al_3Zr and Mg_2Si greatly reduced the grain size and improved the mechanical strength, which resulted in the alloy having comparable properties to 5000 and 6000 series aluminum alloys. Jia *et al.* developed AlMnSc, which is a high strength aluminum alloy, specifically for L-PBF (Jia et al. 2019). The

produced samples have no solidification cracks or obvious metallurgical defects. The strengthening mechanisms of this alloy is also due to precipitation of the secondary phases which triggered *in-situ* heat treatment during L-PBF. Strengthening is also achieved due to the shearing dislocation of these precipitates (Jia et al. 2020). A comparison of tensile properties of this alloy to other aluminum alloys is shown in Figure 2. A comprehensive review on aluminum alloys processed by L-PBF has been done by Aversa *et al.* (Aversa et al. 2019).

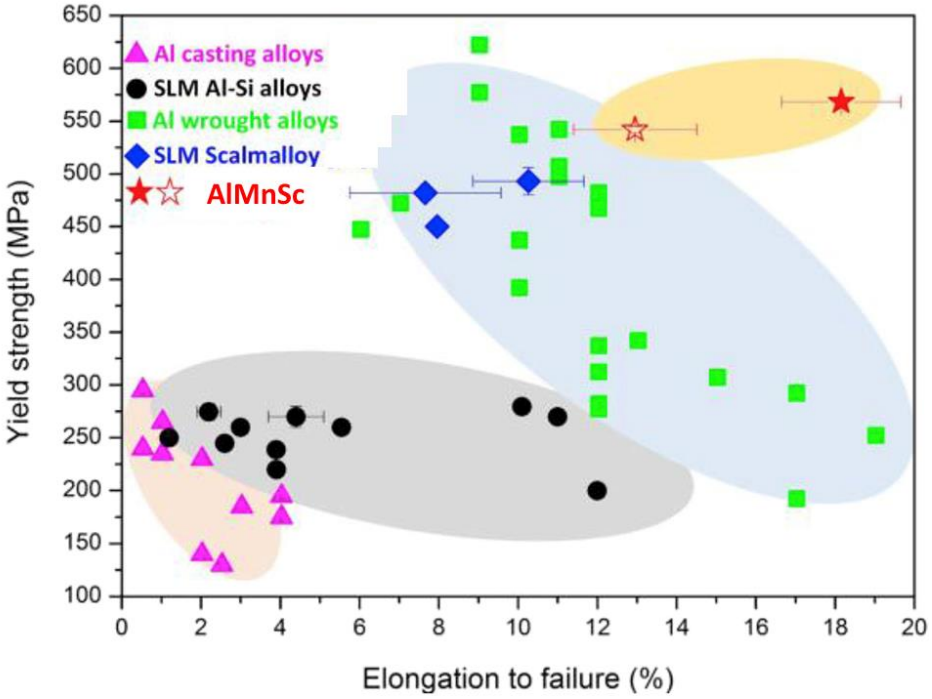

Figure 2 The corresponding tensile properties of AlMnSc alloy tested along horizontal (solid red stars) and vertical (hollow red stars) directions compared with existing typical Al alloys fabricated by both L-PBF and traditional manufacturing processes (Jia et al. 2019).

3.2 High Entropy Alloys

The conventional alloys usually contain one or two primary elements and a relatively small composition of other elements in order to modify their microstructures and properties. In most cases, high entropy alloys (HEAs) are defined as alloys containing five or more major alloying elements with concentration between 5 at% and 35 at%, forming a single or double phase crystalline structure despite having multiple elements with different crystal structures. HEAs

offer good strength to ductility ratio, hardness, corrosion resistance and microstructural flexibility.

Like any other material development using L-PBF, extensive experiments are needed to obtain the process window for these new alloys. Niu *et al.* studied the effect of volumetric energy density on FeMnCoCrNi with emphasis on crack formation mechanisms, crystal orientation and mechanical properties (Niu et al. 2020). Like most conventional alloys, FeMnCoCrNi exhibits crack formations when large thermal stress is generated during L-PBF due to high cooling rate. High cooling rate can be a result of high scanning speed or laser power during L-PBF. Hot tearing is also observed in CoCrFeNi regardless of the various process parameters used, suggesting poor printability of this material by L-PBF (Sun et al. 2019). However, Niu *et al.* also used L-PBF on AlCoCrFeNi (Niu et al. 2019) and achieved a high relative density of 98.4 %. Microstructure of the samples showed epitaxial growth perpendicular to the melt pool boundary. Precipitates which are typically formed after heat treatment are also observed (Sing, Huang, and Yeong 2020). Agrawal *et al.* studied the microstructure and tensile properties of FeMnCoCrSi (CS-HEA) (Agrawal et al. 2020). It is found that the L-PBF FeMnCoCrSi did not contain any cracks and had very small void percentage of ~0.1 vol% which showed the good printability using L-PBF. The ε-dominated columnar grains facilitated the work hardening ability of this material which resulted in very high strength-ductility index. A comparison of CS-HEA and other common alloys strength-ductility index is shown in Figure 3. More details on L-PBF of HEAs are provided in the comprehensive review done by Han *et al.* (Han et al. 2020).

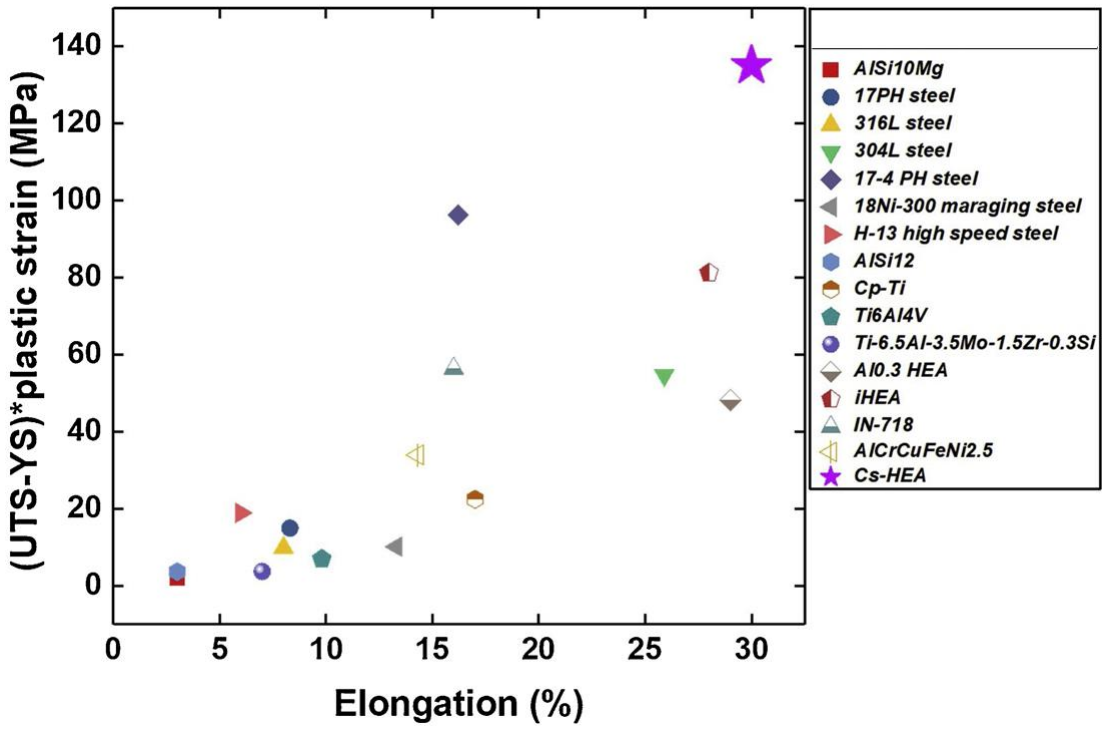

Figure 3 Comparison of strength ductility index as a function of elongation for different additively manufactured alloys (engineering UTS value of all materials is used for calculating SDI) (Agrawal et al. 2020).

3.3 Other New Materials

Other than aluminum alloys and HEAs that have seen a surge in development, there are also some notable work done in shape memory alloys (SMAs) and magnetic alloys.

SMAs are a special group of alloys that can produce mechanical work when subjected to environmental changes such as thermal cycle or magnetic field. Several SMAs have been developed using L-PBF. Among these, NiTi remains a favorite for its super-elasticity, high damping characteristics and lightweight (Chen, Liu, et al. 2019). Lu *et al.* used L-PBF to produce NiTi that has extremely high shape memory effect of 98.7 % recovery ratio and 4.99 % recoverable strain after ten loading-unloading cycle (Lu et al. 2019). The strengthening mechanism is attributed to lack of defects, grain refinement strengthening and the nano sized Ti_2Ni precipitates formed. Furthermore, Xiong *et al.* reported a 99 % shape recovery rate when L-PBF NiTi thin walls are compressively deformed by 50 % (Figure 4) (Xiong et al. 2019).

Other than NiTi, some other SMAs that have been processed using L-PBF including TiNbZrMoSn (Liu, Zhang, and Zhang 2019), TiNbTaZr (Hafeez et al. 2020), CuZnAl (Zhou et al. 2020), CoNiGa (Lauhoff et al. 2020) and CuAlNiTi (Tian et al. 2019).

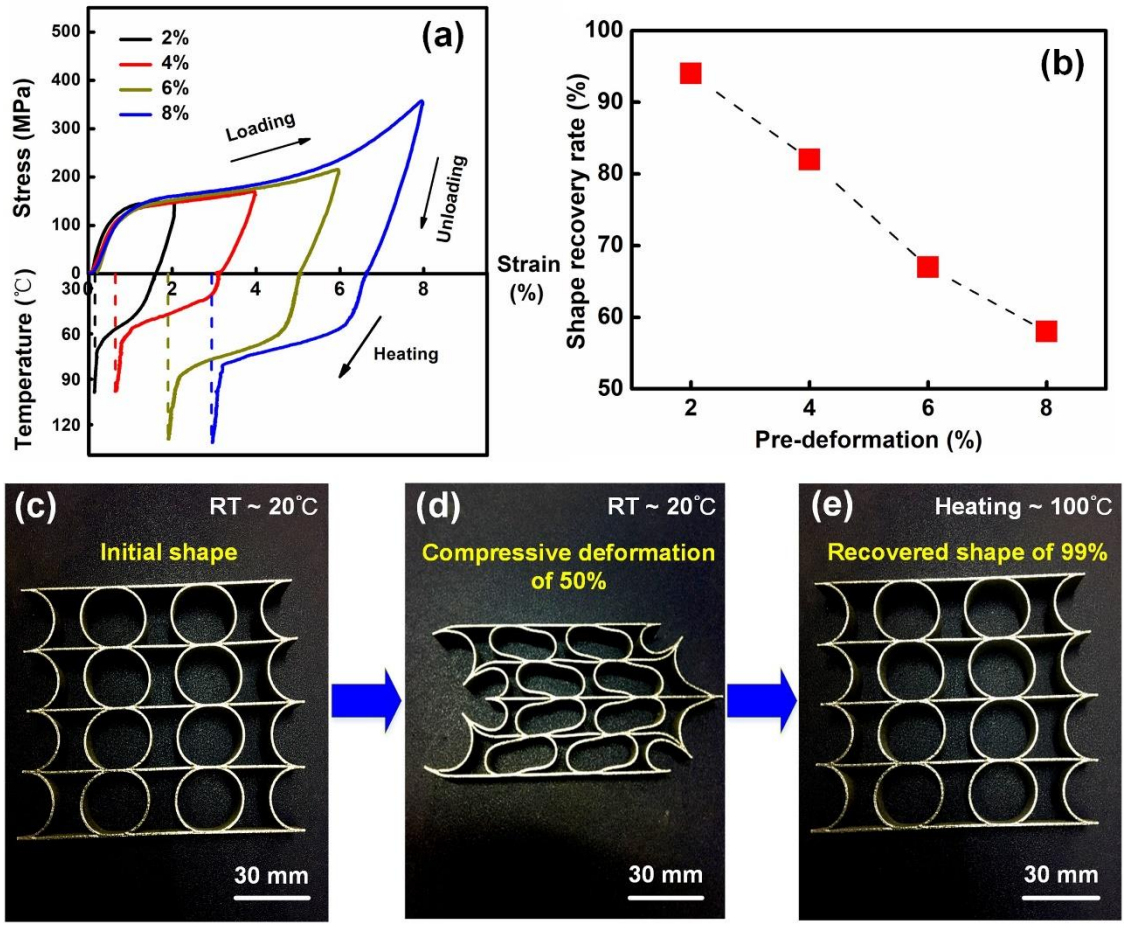

Figure 4 (a) Stress-Strain-Temperature curves obtained by tensile loading-unloading-heating process of the L-PBF NiTi (b) shape recovery rate as a function of tensile pre-deformation (c) the initial shape of printed L-PBF NiTi part (d) the compressed L-PBF NiTi part with deformation of 50% and (e) the recovered shape of the L-PBF NiTi part after heating (Xiong et al. 2019).

Research on magnetic alloys by L-PBF is still in infancy stage. Goll *et al.* investigated the processing of FeNdB using L-PBF and showed that very fine microstructure with defined texture and finely dispersed neodymium rich phase is formed. However, they concluded that further process parameters optimization is needed to achieve finer microstructure for better performance (Goll, Vogelgsang, et al. 2019). Mohamed *et al.* created dense NiFeMo (relative density of 98.9

%) structures using L-PBF and tried to control the crystallographic anisotropy (Mohamed et al. 2020). In another work, Bittner *et al.* used L-PBF to produce NdFeB magnets and were able to achieve isotropy (Bittner, Thielsch, and Drossel 2020). In addition, it is found that the magnetic properties become better as energy input increases until the material specific threshold have been reached for 3D printability. The grain size and density of the samples are identified as the main factors in affecting the magnetic properties. Similar observations were made by Skalon *et al.* who studied the influence of melt pool stability on NdFeB magnets density and magnetic properties (Skalon et al. 2020). In addition, it has been showed that topological optimization made possible by L-PBF has improved their performance (Figure 5) (Goll, Schuller, et al. 2019).

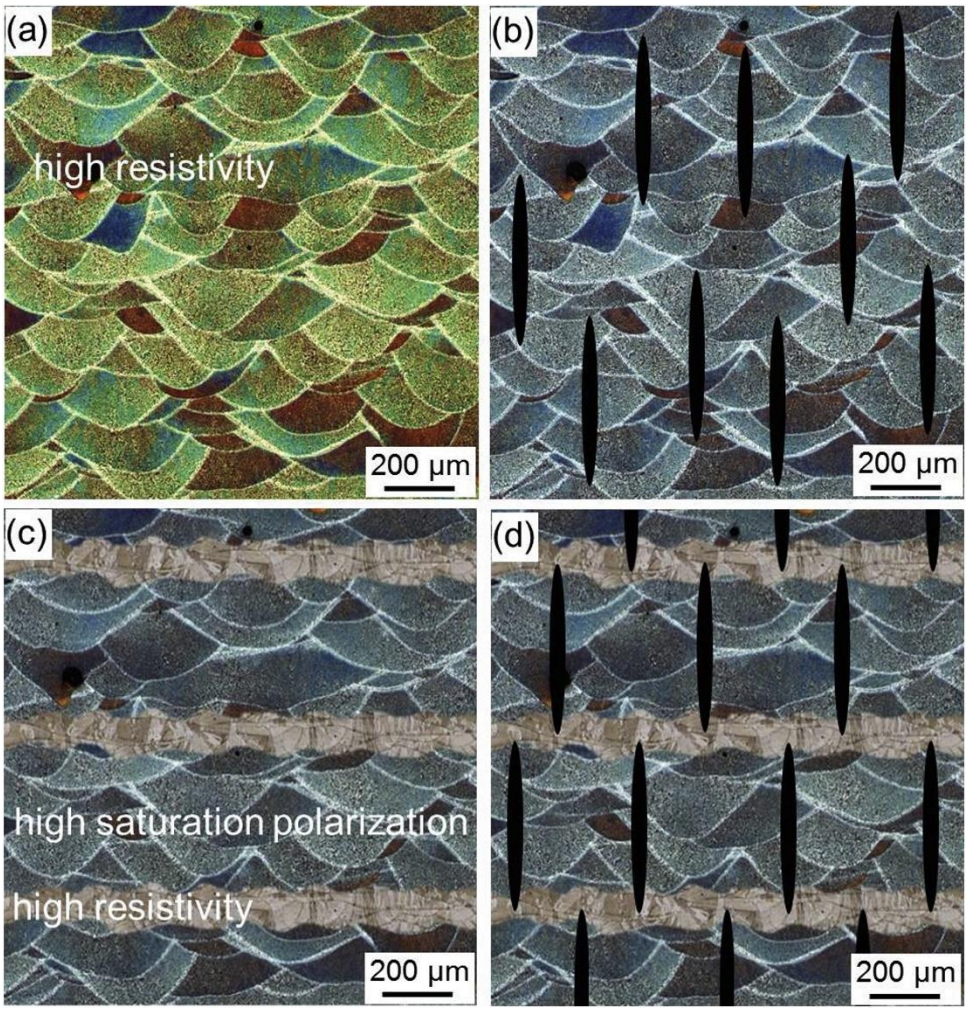

Figure 5 Schematic representation of different concepts to reduce eddy current losses of soft magnetic cores by additive manufacturing (a) Optimized alloy composition with higher electrical resistivity and better soft magnetic properties (large saturation polarization, large permeability) (b) novel topological structures (c) layered structures to design and control electrical path length and magnetic flux and (d) combination thereof (Goll, Schuller, et al. 2019).

4. Recent Process Development for Laser Powder Bed Fusion

In addition to materials development, there is also significant progress in the process for L-PBF. Currently, much of the adoption of L-PBF for industry is hindered by obstacles such as part quality and process efficiency. Majority of the research done has focused on the process parameters to improve L-PBF parts. To further enhance the feasibility of L-PBF for actual manufacturing and integration into the process chains, the recent key process advancements for L-PBF are discussed.

4.1 Scanning Strategies

Remelting, which refers to scanning the powder layer more than once (Figure 6), during L-PBF has emerged as a popular option in improving the part quality such as density and surface finishing. Remelting is also referred as *in-situ* heat treatment which results in reduced thermal stress and inhibits crack initiation and propagation. Hence, this scanning strategy has potential for materials with low 3D printability with L-PBF.

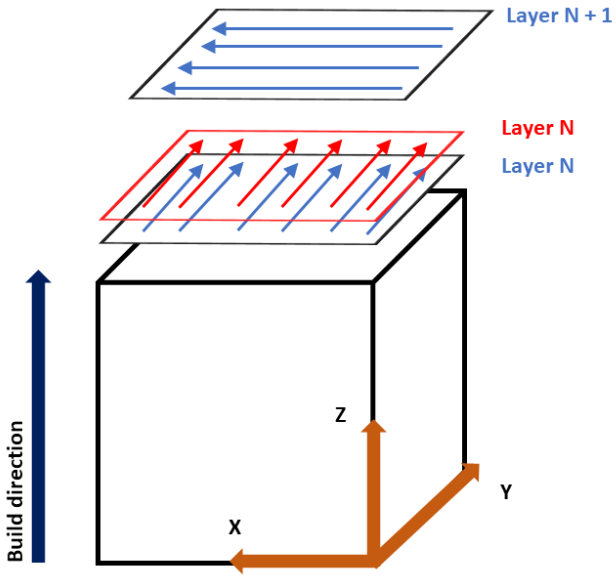

Figure 6 Schematic of remelting during L-PBF.

Xiong *et al.* used remelting to process pure tungsten by L-PBF and found that the grain size and defects are reduced (Xiong et al. 2020). It is of interest to note that the remelting does not need to have the same process parameters or scan directions as the first scanning. This allows for more variable in terms of parameters optimization. Yu *et al.* also concluded that porosity reduces with remelting, however, remelting in opposite scan direction results in lower reduction in porosity at the part edges compared to remelting in the same direction (Yu, Sing, Chua, and Tian 2019).

In addition to remelting, much of the development in scanning strategies for L-PBF is in the design of scanning patterns. Currently, the scanning patterns used in L-PBF include stripes and chessboard or island in which the layer cross sections are divided into smaller areas (Figure 7). It has been shown that scanning patterns have effect on the residual stresses of L-PBF parts (Li et al. 2018). In attempts to reduce the residual stresses in L-PBF parts, several modifications to the patterns have been developed.

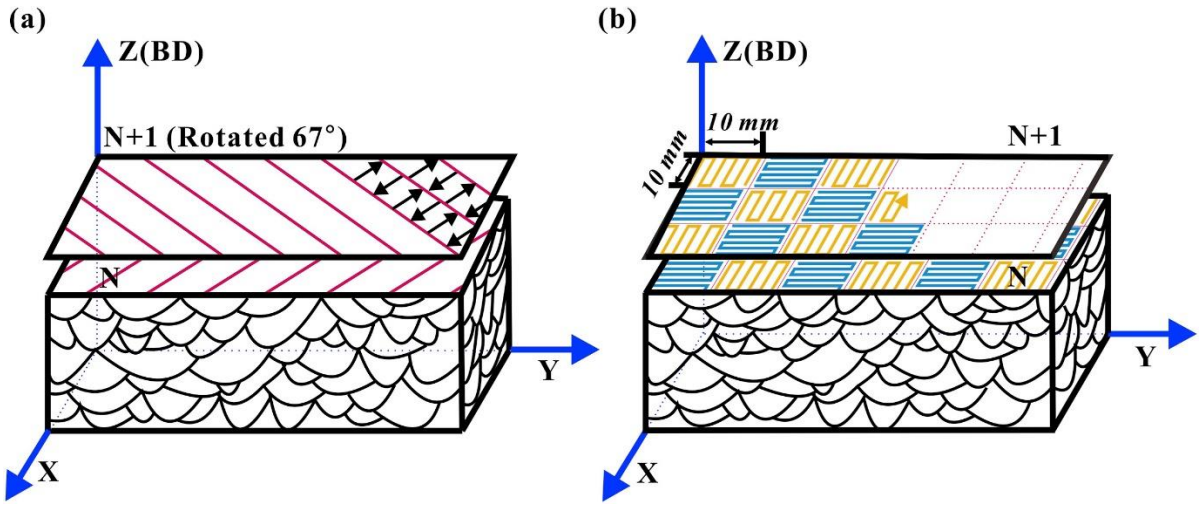

Figure 7 Schematic illustration of two scanning strategies (a) stripe and (b) chessboard (Wang, Lei, et al. 2020).

To improve the chessboard scanning pattern, Ramos *et al.* proposed an intermittent scanning pattern where the alternating areas are not scanned adjacently. Using simulations, it is shown that this is effective in reducing the residual stresses due to the shorter scan vector lengths (Ramos, Belblidia, and Sienz 2019). The scan rotation between each layer is also found to have effect on the microstructure and mechanical properties of L-PBF parts. The scan rotation can be set at any angle, and some examples are shown in Figure 8.

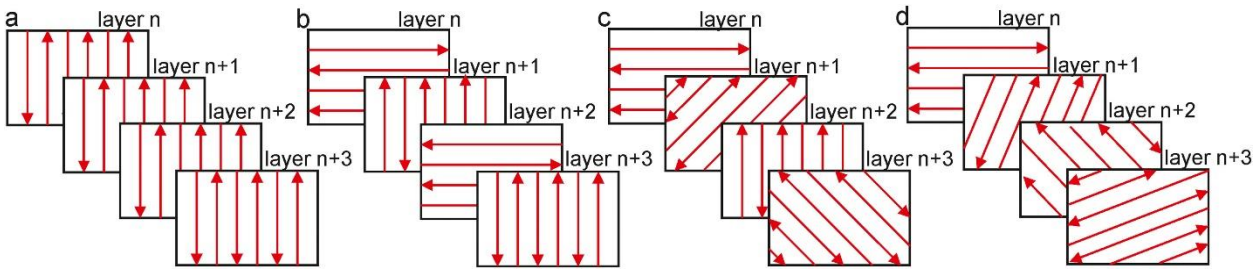

Figure 8 Schematic overview of the laser vectors (red arrows) with a bidirectional scanning strategy with (a) no rotation (b) 90° rotation, (c) 45° rotation and (d) 67° rotation on subsequent layers (n) (Leicht et al. 2020).

Using bidirectional scanning in each layer (Figure 8), Leicht *et al.* found that scan rotation does not affect part density if the melt pools have sufficient overlaps in width and height. However, samples produced with no rotation had the highest tensile strength but lowest hardness, showing anisotropy (Leicht et al. 2020). Similar observations were made by Wan *et al.* and Liu *et al.* that showed that samples produced with no scan rotation are stronger than samples that used 90 ^{o} scan rotation despite no difference in parts porosity (Wan et al. 2019; Liu et al. 2019). With island scanning pattern, there are also more variables in scan pattern designs. Chen *et al.* studied the effect of overlap amount and patterns using island scanning (Chen, Yin, et al. 2019). It is interesting to note that the overlap region experiences remelting due to the scanning of the region twice. Hence, increasing the overlap region area resulted in higher stress relief for all the scanning patterns.

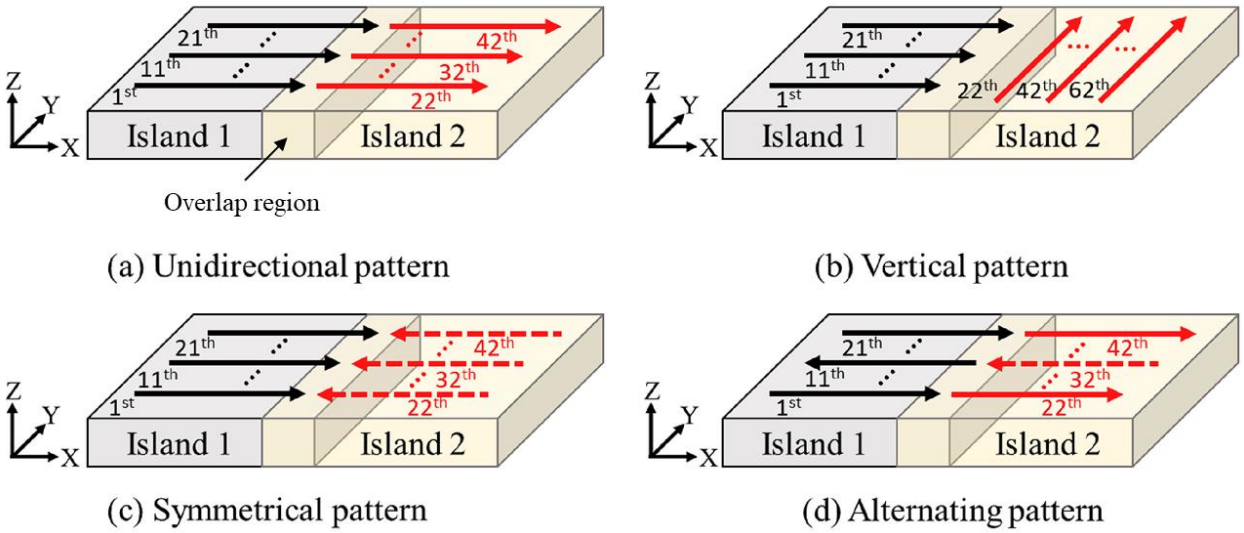

Figure 9 The overlap patterns used in the scanning region (a) unidirectional (b) vertical (c) symmetrical (d) alternating (Chen, Yin, et al. 2019).

The study on overlap regions is useful for the development of multi-lasers L-PBF.

4.2 Multi-lasers

Using multi-lasers in L-PBF can increase the production rate and by allowing more than one unit of laser, the laser properties will have more freedom, such as different laser spot sizes for different geometrical features and resolutions.

Zhang *et al.* used multi-lasers L-PBF to study the effect of overlap on defects, microstructure and mechanical properties of AlSi10Mg. The build substrate is divided into four areas where there is overlap of 1 mm between each quadrant which experienced remelting (Figure 10). Samples placed in the overlap have similar microstructure and tensile strength as compared with other samples (Zhang et al. 2019).

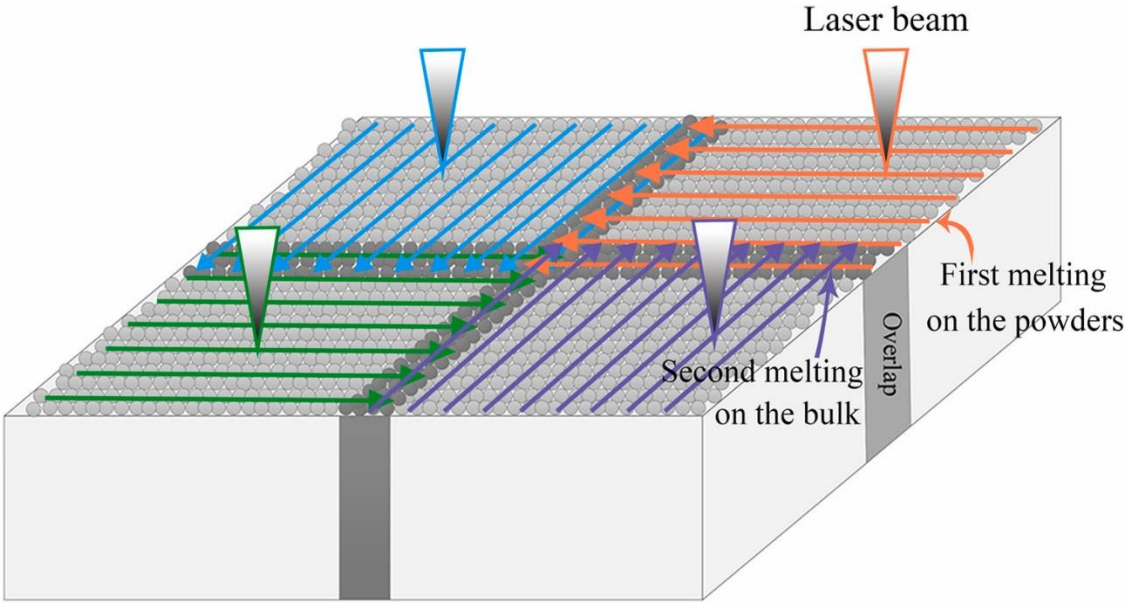

Figure 10 Schematic of the overlap area melt in multi-lasers L-PBF (Zhang et al. 2019).

It is concluded that multi-lasers L-PBF has higher build rate compared to single laser without compromising part density or changing the microstructure drastically (Wong et al. 2019). Instead of installing additional laser units, Tsai *et al.* used a diffractive optical element and galvanometric scanner to create multiple spots from a single laser L-PBF. This also allowed adjustment of individual laser spot characteristics (Tsai et al. 2019).

4.3 Other Process Considerations and Developments

There are several other process aspects of development for L-PBF, such as auto generation of build orientation (Qin et al. 2020) and support structure designs. These advances aim to achieve higher industry readiness for L-PBF. For this to be attained, there are also other considerations.

Shielding gases are often used in L-PBF to prevent oxidation and containments pick up by the materials. However, there is need for further understanding of the effect of such gases on the L-PBF parts. A graphic description of the gas flow interactions with spatter from the melt pools is shown in Figure 11.

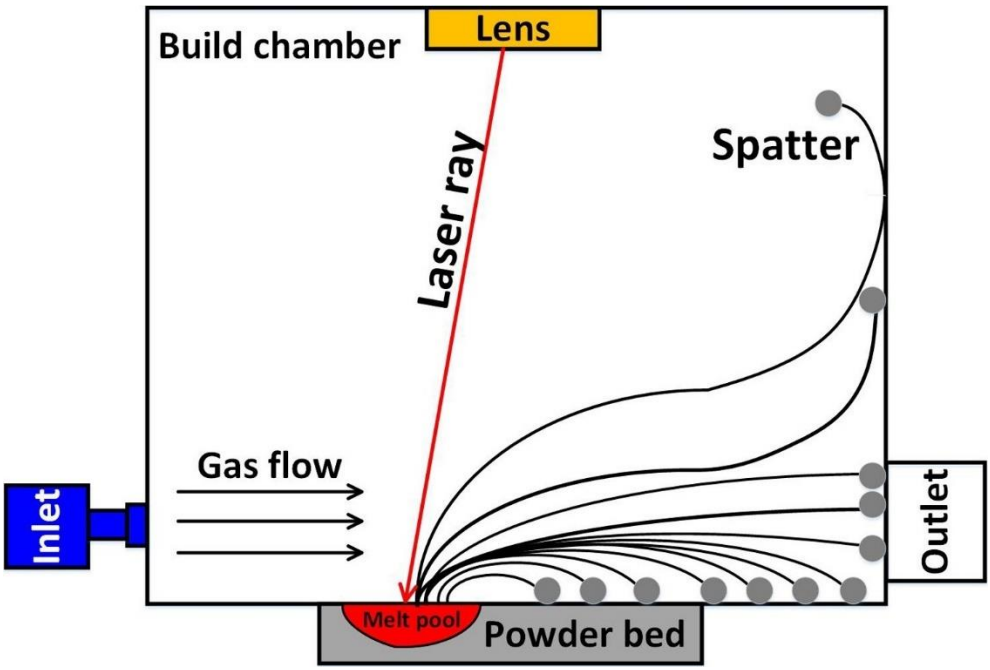

Figure 11 Graphic description of the LPBF process chamber and the spatter/gas flow interactions (Zhang, Cheng, and Tuffile 2020).

Anwar *et al.* investigated the distribution of spatter due to the gas flow. It is shown that the gas flow was not effective in removing the larger spatter particles (Anwar, Ibrahim, and Pham 2019). In addition, Zhang *et al.* considered the effect of the gas flow in removal of the emissions from melt pools (Zhang, Cheng, and Tuffile 2020). It is observed that there is a downward flow tendency for the gas flow, and an additional row of gas nozzles is placed directly under the original nozzles to prevent this. The new design improved the spatter removal rate from 69 % to 93 %. Puazon *et al.* investigated the effect of the shielding gas thermal properties on the Ti6Al4V part density produced using L-PBF (Puazon et al. 2020). Mixtures of helium and argon gases are used, instead of pure argon, as helium has high thermal conductivity and heat capacity. It is showed that using argon and helium mixtures, the build rate can increase up to 40 % while ensuring process stability and producing parts with full density. The capability of increase build rate is attributed to better spatter removal and cooling rates even when higher powers and

scanning speeds are used. Similar observations were made by Caballero *et al.* when pure helium was used instead of argon. It is observed that the strong fluctuations in melting is absence in helium atmosphere, and better control of the melt profiles was achieved compared to argon (Caballero et al. 2020). However, for AlSi10Mg, there is no significant difference observed when nitrogen was used instead of argon (Ch et al. 2019).

Despite the forming of spatter and condensate during L-PBF (Figure 12), which can result in change in powder characteristics, recycling is commonly carried out for the powder.

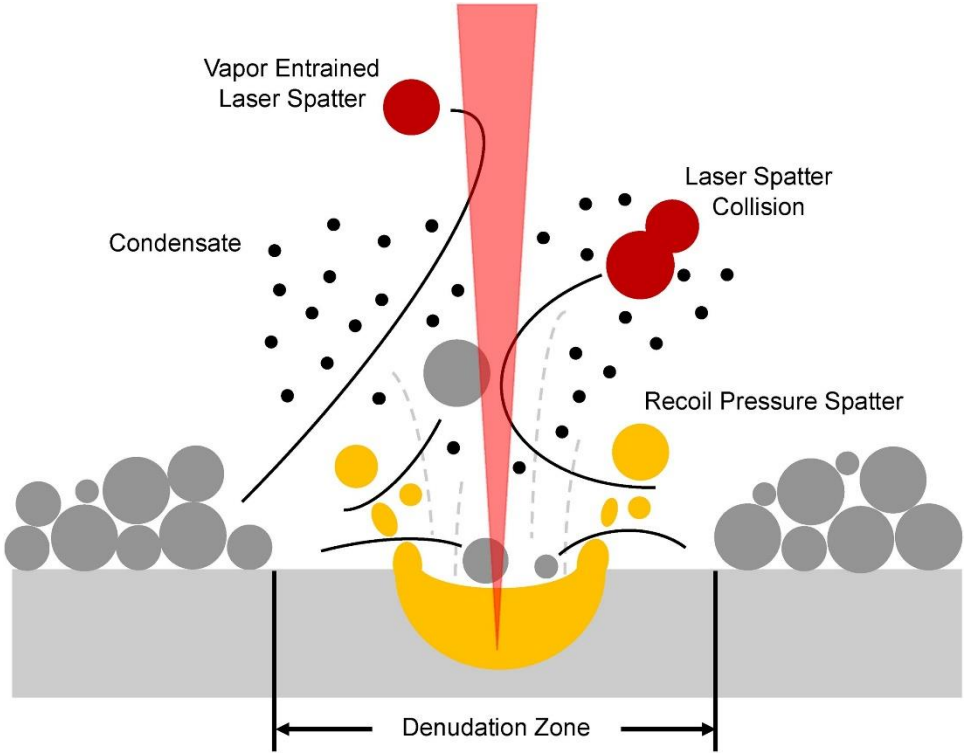

Figure 12 Illustration of laser spatter and condensate formation during the L-PBF process. Laser spatter is formed as a result of recoil pressure or vapor entrainment and is ejected away from the melt pool into the surrounding powder bed affecting powder recyclability (Sutton et al. 2020).

Several researches have been done to study the effect of reusing powders for L-PBF. Carrion *et al.* studied the effect on mechanical properties by reusing Ti6Al4V powders for L-PBF (Carrion et al. 2019). While the powder has narrower powder size distribution (PSD) after 15

cycles of recycling, which leads to increase in powder flowability, the L-PBF parts produced did no show significant changes in microstructure, tensile and fatigue performance. Similar results are obtained by Alamos *et al.* after eight recycling (Alamos et al. 2020). Using 304L stainless steel powder that has been recycled for seven times, Sutton *et al.* also observed narrower PSD and better flowability due to the loss of finer powder particles, but the recycled powder particles have higher oxygen content and a change in microstructure (Sutton et al. 2020). Higher oxygen content was also observed for AlSi10Mg powder after recycling 16 times (Cordova, Campos, and Tinga 2019). Higher oxygen content is attributed to contamination pick up and element vaporization. Wang *et al.* observed a decrease in mechanical properties of CoCrW parts formed by L-PBF using powder that has been recycled six time (Wang, Ye, et al. 2020). A review on powder recycling has been done by Powell *et al.* (Powell et al. 2020).

5. Concluding Remarks

L-PBF, with its better resolutions and capabilities in manufacturing functional parts, have seen recent advancements driven by the demand from industries. In this perspective article, the recent developments in L-PBF are highlighted from the materials and process points of view. However, there are still many potential and challenges faced by this technique which open many research opportunities. For materials, there are still challenges faced in designing new alloys specifically for L-PBF as there is need to overcome metallurgical defects such as pores, lack of fusion and intermetallic formations. These are commonly caused by L-PBF and have detrimental effects on the parts performance. Thus, in-depth understanding of the process is essential. For the L-PBF process, many applications are faced with the uncertainty and unpredictability of the process. These are attributed to the lack of process control solutions available in the market. Developing machine learning techniques and artificial intelligence to complement the existing

numerical simulations can aid in the development of in-process and post-process monitoring systems.

Acknowledgement

The authors acknowledge the support from the National Research Foundation, Prime Minister's Office, Singapore under its Medium-Sized Centre funding scheme.

References

Agrawal, P., S. Thapliyal, S. S. Nene, R. S. Mishra, B. A. McWilliams, and K. C. Cho. 2020. "Excellent strength-ductility synergy in metastable high entropy alloy by laser powder bed additive manufacturing." *Additive Manufacturing* 32:101098.

Alamos, Fernando J., Jessica Schiltz, Kristen Kozlovsky, Ross Attardo, Charles Tomonto, Tom Pelletiers, and Steven R. Schmid. 2020. "Effect of powder reuse on mechanical properties of Ti-6Al-4V produced through selective laser melting." *International Journal of Refractory Metals and Hard Materials* 91:105273.

Anwar, Ahmad Bin, Imran Halimi Ibrahim, and Quang-Cuong Pham. 2019. "Spatter transport by inert gas flow in selective laser melting: A simulation study." *Powder Technology* 352:103-16.

Aversa, Alberta, Giulio Marchese, Abdollah Saboori, Emilio Bassini, Diego Manfredi, Sara Biamino, Daniele Ugues, Paolo Fino, and Mariangela Lombardi. 2019. "New Aluminum Alloys Specifically Designed for Laser Powder Bed Fusion: A Review." *Materials* 12 (7):1007.

Bi, Jiang, Zhenglong Lei, Yanbin Chen, Xi Chen, Ze Tian, Jingwei Liang, Xikun Qin, and Xinrui Zhang. 2020. "Densification, microstructure and mechanical properties of an Al-

14.1Mg-0.47Si-0.31Sc-0.17Zr alloy printed by selective laser melting." *Materials Science and Engineering: A* 773:138931.

Bi, Jiang, Zhenglong Lei, Yanbin Chen, Xi Chen, Ze Tian, Xikun Qin, Jingwei Liang, and Xinrui Zhang. 2020. "Effect of Al3(Sc, Zr) and Mg2Si precipitates on microstructure and tensile properties of selective laser melted Al-14.1Mg-0.47Si-0.31Sc-0.17Zr alloy." *Intermetallics* 123:106822.

Bittner, Florian, Juliane Thielsch, and Welf-Guntram Drossel. 2020. "Laser powder bed fusion of Nd–Fe–B permanent magnets." *Progress in Additive Manufacturing* 5:3-9.

Blindheim, Jorgen, Torgeir Welo, and Martin Steinert. 2019. "First demonstration of a new additive manufacturing process based on metal extrusion and solid-state bonding." *The International Journal of Advanced Manufacturing Technology* 105:2523-30.

Bogue, Robert. 2011. "Nanocomposites: a review of technology and applications." *Assembly Automation* 31 (2):106-12.

Buchanan, C., and L. Gardner. 2019. "Metal 3D printing in construction: A review of methods, research, applications, opportunities and challenges." *Engineering Structures* 180:332-48.

Caballero, Armando, Wojciech Suder, Xin Chen, Goncalo Pardal, and Stewart Williams. 2020. "Effect of shielding conditions on bead profile and melting behaviour in laser powder bed fusion additive manufacturing." *Additive Manufacturing*.

Carrion, Patricio E., Arash Soltani-Tehrani, Nam Phan, and Nima Shamsaei. 2019. "Powder Recycling Effects on the Tensile and Fatigue Behavior of Additively Manufactured Ti-6Al-4V Parts." *JOM* 71:963-73.

Ch, Srinivasa Rakesh, A. Raja, Priyanka Nadig, R. Jayaganthan, and N. J. Vasa. 2019. "Influence of working environment and built orientation on the tensile properties of selective laser melted AlSi10Mg alloy." *Materials Science and Engineering: A* 750:141-51.

Chahal, Vedant, and Robert M. Taylor. 2020. "A review of geometric sensitivities in laser metal 3D printing." *Virtual and Physical Prototyping* 15 (2):227-41.

Chen, Changpeng, Jie Yin, Haihong Zhu, Zhongxu Xiao, Luo Zhang, and Xiaoyan Zeng. 2019. "Effect of overlap rate and pattern on residual stress in selective laser melting." *International Journal of Machine Tools and Manufacture* 145:103433.

Chen, Xizhang, Kun Liu, Wei Guo, Namrata Gangil, Arshad Noor Siddiquee, and Sergey Konovalov. 2019. "The fabrication of NiTi shape memory alloy by selective laser melting: a review." *Rapid Prototyping Journal* 25 (8):1421-32.

Concli, Franco, and Andrea Giliolo. 2019. "Numerical and experimental assessment of the mechanical properties of 3D printed 18-Ni300 steel trabecular structures produced by Selective Laser Melting – a lean design approach." *Virtual and Physical Prototyping* 14 (3):267-76.

Cordova, Laura, Monica Campos, and Tiedo Tinga. 2019. "Revealing the Effects of Powder Reuse for Selective Laser Melting by Powder Characterization." *JOM* 71:1062-72.

DebRoy, T., H. L. Wei, J. S. Zuback, T. Mukherjee, J. W. Elmer, J. O. Milewski, A. M. Beese, A. Wilson-Heid, A. De, and W. Zhang. 2018. "Additive manufacturing of metallic components – Process, structure and properties." *Progress in Materials Science* 92:112-224. doi: 10.1016/j.pmatsci.2017.10.001.

Dikshit, V., A. P. Nagalingam, Y. L. Yap, S. L. Sing, W. Y. Yeong, and J. Wei. 2018. "Crack monitoring and failure investigation on inkjet printed sandwich structures under quasi-static indentation test." *Materials & Design* 137:140-51.

Dikshit, V., A. Nagalingam, Y. L. Yap, S. L. Sing, W. Y. Yeong, and J. Wei. 2017. "Investigation of quasi-static indentation response of inkjet printed sandwich structures under various indenter geometries." *Materials* 10 (3):290.

Du, Z., H. C. Chen, M. J. Tan, G. Bi, and C. K. CHua. 2020. "Effect of nAl2O3 on the part density and microstructure during the laser-based powder bed fusion of AlSi10Mg composite." *Rapid Prototyping Journal* 26 (4):727-35.

Eisenbarth, Daniel, Fabian Soffel, and Konrad Wegener. 2019. "Effects of direct metal deposition combined with intermediate and final milling on part distortion." *Virtual and Physical Prototyping* 14 (2):130-4.

Galante, Raquel, Celio G. Figueiredo-Pina, and Ana Paula Serro. 2019. "Additive manufacturing of ceramics for dental applications: A review." *Dental Materials* 35 (6):825-46.

Gisario, Annamaria, Michele Kazarian, Filomeno Martina, and Mehrshad Mehrpouya. 2019. "Metal additive manufacturing in the commerical aviation industry: A review." *Journal of Manufacturing Systems* 53:124-49.

Goh, G. D., Y. L. Yap, H. K. J. Tan, S. L. Sing, G. L. Goh, and W. Y. Yeong. 2020. "Process–structure–properties in polymer additive manufacturing via material extrusion: A review." *Critical Reviews in Solid State and Materials Sciences* 45 (2):113-33.

Goll, D., D. Schuller, G. Martinek, T. Kunert, J. Schurr, C. Sinz, T. Schubert, T. Bernthaler, H. Riegel, and G. Schneider. 2019. "Additive manufacturing of soft magnetic materials and components." *Additive Manufacturing* 27:428-39.

Goll, Dagmar, David Vogelgsang, Ulrich Pflanz, Dominic Hohs, Tvrtko Grubesa, Julian Schurr, Timo Bernthaler, David Kolb, Harald Riegel, and Gerhard Schneider. 2019. "Refining the Microstructure of Fe-Nd-B by Selective Laser Melting." *Physica Status Solidi Rapid Research Letter* 13:1800536.

Gu, D. D., W. Meiners, K. Wissenbach, and R. Poprawe. 2013. "Laser additive manufacturing of metallic components: materials, processes and mechanisms." *International Materials Reviews* 57 (3):133-64. doi: 10.1179/1743280411y.0000000014.

Guo, Meng, Dongdong Gu, Lixia Xi, Lei Du, Hongmei Zhang, and Jiayao Zhang. 2019. "Formation of scanning tracks during Selective Laser Melting (SLM) of pure tungsten powder: Morphology, geometric features and forming mechanisms." *International Journal of Refractory Metals and Hard Materials* 79:37-46.

Hafeez, Noman, Jia Liu, Liqiang Wang, Daixiu Wei, Yujin Tang, Weijie Lu, and Lai-Chang Zhang. 2020. "Superelastic response of low-modulus porous beta-type Ti-35Nb-2Ta-3Zr alloy fabricated by laser powder bed fusion." *Additive Manufacturing* 34:101264.

Han, Changjun, Qihong Fang, Yusheng Shi, Shu Beng Tor, Chee Kai Chua, and Kun Zhou. 2020. "Recent Advances on High-Entropy Alloys for 3D Printing." *Advanced Materials*:1903855.

Huang, Sheng, Swee Leong Sing, Geoff de Looze, Robert Wilson, and Wai Yee Yeong. 2020. "Laser powder bed fusion of titanium-tantalum alloys: Compositions and designs for biomedical applications." *Journal of the Mechanical Behavior of Biomedical Materials* 108:103775.

Jia, Qingbo, Paul Rometsch, Philipp Kurnsteiner, Qi CHao, Aijun Huang, Matthew Weyland, Laure Bourgeois, and Xinhua Wu. 2019. "Selective laser melting of a high strength Al-Mn-Sc alloy: Alloy design and strengthening mechanisms." *Acta Materialia* 171:108-18.

Jia, Qingbo, Fan Zhang, Paul Rometsch, Jingwei Li, Jitendra Mata, Matthew Weyland, Laure Bourgeois, Manling Sui, and Xinhua Wu. 2020. "Precipitation kinetics, microstructure evolution and mechanical behavior of a developed Al–Mn–Sc alloy fabricated by selective laser melting." *Acta Materialia* 193:239-51.

Kuo, C. N., C. K. Chua, P. C. Peng, Y. W. Chen, S. L. Sing, S. Huang, and Y. L. Su. 2020. "Microstructure evolution and mechanical property response via 3D printing parameter development of Al–Sc alloy." *Virtual and Physical Prototyping* 15 (1):120-9.

Lauhoff, C., A. Fischer, C. Sobrero, A. Liehr, P. KrooB, F. Brenne, J. Richter, M. Kahlert, S. Bohm, and T. Niendorf. 2020. "Additive Manufacturing of Co-Ni-Ga High-Temperature Shape Memory Alloy: Processability and Phase Transformation Behavior." *Metallurgical and Materials Transactions A* 51:1056-61.

Lee, J. M., S. L. Sing, M. Zhou, and W. Y. Yeong. 2018. "3D bioprinting processes: A perspective on classification and terminology." *International Journal of Bioprinting* 4 (2):151.

Leicht, A., C. H. Yu, V. Luzin, U. Klement, and E. Hryha. 2020. "Effect of scan rotation on the microstructure development and mechanical properties of 316L parts produced by laser powder bed fusion." *Materials Characterization* 163:110309.

Li, Yingli, Kun Zhou, Pengfei Tan, Shu Beng Tor, Chee Kai Chua, and Kah Fai Leong. 2018. "Modeling temperature and residual stress fields in selective laser melting." *International Journal of Mechanical Sciences* 136:24-35.

Liu, C. Y., J. D. Tong, M. G. Jiang, Z. W. Chen, G. XU, H. B. Liao, P. Wang, X. Y. Wang, M. Xu, and C. S. Lao. 2019. "Effect of scanning strategy on microstructure and mechanical properties of selective laser melted reduced activation ferritic/martensitic steel." *Materials Science and Engineering: A* 766:138364.

Liu, Y. J., Y. S. Zhang, and L. C. Zhang. 2019. "Transformation-induced plasticity and high strength in beta titanium alloy manufactured by selective laser melting." *Materialia* 6:100299.

Liu, Z. H., D. Q. Zhang, S. L. Sing, C. K. Chua, and L. E. Loh. 2014. "Interfacial characterization of SLM parts in multi-material processing: Metallurgical diffusion between 316L stainless steel and C18400 copper alloy." *Materials Characterization* 94:116-25.

Loh, Loong Ee, Chee Kai Chua, Wai Yee Yeong, Jie Song, Mahta Mapar, Swee Leong Sing, Zhong Hong Liu, and Dan Qing Zhang. 2015. "Numerical investigation and an effective modelling on the Selective Laser Melting (SLM) process with aluminium alloy 6061." *International Journal of Heat and Mass Transfer* 80:288-300.

Lores, Asier, Naiara Azurmendi, Inigo Agote, and Ester Zuza. 2019. "A review on recent developments in binder jetting metal additive manufacturing: materials and process characteristics." *Powder Metallurgy* 62 (5):267-96.

Lu, Z. H., C. Yang, X. Luo, H. W. Ma, B. Song, Y. Y. Li, and L. C. Zhang. 2019. "Ultrahigh-performance TiNi shape memory alloy by 4D printing." *Materials Science and Engineering: A* 763:138166.

Martinez, Rafael, Iain Todd, and Kamran Mumtaz. 2019. "In situ alloying of elemental Al-Cu12 feedstock using selective laser melting." *Virtual and Physical Prototyping* 14 (3):242-52.

Mohamed, Abd El-Moez A., Ji Zou, Richard S. Sheridan, Kai Bongs, and Moataz M. Attallah. 2020. "Magnetic shielding promotion via the control of magnetic anisotropy and thermal Post processing in laser powder bed fusion processed NiFeMo-based soft magnet." *Additive Manufacturing* 32:101079.

Niu, P. D., R. D. Li, T. C. Yuan, S. Y. Zhu, C. Chen, M. B. Wang, and L. Huang. 2019. "Microstructures and properties of an equimolar AlCoCrFeNi high entropy alloy printed by selective laser melting." *Intermetallics* 104:24-32.

Niu, Pengda, Ruidi Li, Shuya Zhu, Minbo Wang, Chao Chen, and Tiechui Yuan. 2020. "Hot cracking, crystal orientation and compressive strength of an equimolar CoCrFeMnNi high-entropy alloy printed by selective laser melting." *Optics & Laser Technology* 127:106147.

Olakanmi, E. O., R. F. Cochrane, and K. W. Dalgarno. 2015. "A review on selective laser sintering/melting (SLS/SLM) of aluminium alloy powders: Processing, microstructure, and properties." *Progress in Materials Science* 74:401-77. doi: 10.1016/j.pmatsci.2015.03.002.

Olivier, D., J. A. Travieso-Rodriguez, S. Borros, G. Reyes, and R. Jerez-Mesa. 2017. "Influence of building orientation on the flexural strength of laminated object manufacturing specimens." *Journal of Mechanical Science and Technology* 31:133-9.

Powell, Daniel, Allan Rennie, Louise Geekie, and Neil Burns. 2020. "Understanding powder degradation in metal additive manufacturing to allow the upcycling of recycled powders." *Journal of Cleaner Production*:122077.

Puazon, Camille, Pierre Foret, Eduard Hryha, Tanja Arunprasad, and Lars Nyborg. 2020. "Argon-helium mixtures as Laser-Powder Bed Fusion atmospheres: Towards increased build rate of Ti-6Al-4V." *Journal of Materials Processing Technology* 279:116555.

Qin, Yuchu, Qunfen Qi, Peizhi Shi, Paul J. Scott, and Xiangqian Jiang. 2020. "Automatic generation of alternative build orientations for laser powder bed fusion based on facet clustering." *Virtual and Physical Prototyping*.

Ramos, Davi, Fawzi Belblidia, and Johann Sienz. 2019. "New scanning strategy to reduce warpage in additive manufacturing." *Additive Manufacturing* 28:554-64.

Sercombe, T. B., and X. Li. 2016. "Selective laser melting of aluminium and aluminium metal matrix composites: a review." *Materials Technology* 31 (2):77-85.

Shuai, Cijun, Chongxian He, Liang Xu, Quan Li, Tong Chen, Youwen Yang, and Shuping Peng. 2018. "Wrapping effect of secondary phases on the grains: increased corrosion resistance of Mg–Al alloys." *Virtual and Physical Prototyping* 13 (4).

Shuai, Cijun, Lianfeng Xue, Chengde Gao, Youwen Yang, Shuping Peng, and Yanru Zhang. 2018. "Selective laser melting of Zn–Ag alloys for bone repair: microstructure, mechanical properties and degradation behaviour." *Virtual and Physical Prototyping* 13 (3):146-54.

Shuai, Cijun, Wenjing Yang, Youwen Yang, Chengde Gao, Chongxian He, and Hao Pan. 2019. "A continuous net-like eutectic structure enhances the corrosion resistance of Mg alloys." *International Journal of Bioprinting* 5 (2):207.

Simonelli, Marco, Nesma Aboulkhair, Mircea Rasa, Mark East, Chris Tuck, Ricky Wildman, Otto Salomons, and Richard Hague. 2019. "Towards digital metal additive manufacturing via high-temperature drop-on-demand jetting." *Additive Manufacturing* 30:100930.

Sing, S. L., W. Y. Yeong, F. E. Wiria, B. Y. Tay, Z. Zhao, L. Zhao, Z. Tian, and S. Yang. 2017. "Direct selective laser sintering and melting of ceramics: a review." *Rapid Prototyping Journal* 23 (3):611-23.

Sing, Swee Leong, Sheng Huang, and Wai Yee Yeong. 2020. "Effect of solution heat treatment on microstructure and mechanical properties of laser powder bed fusion produced cobalt-28chromium-6molybdenum." *Materials Science and Engineering: A* 769:138511.

Skalon, Mateusz, Michael Gortler, Benjamin Meier, Siegfried Arneitz, Nikolaus Urban, Stefan Mitsche, Christian Huber, Joerg Franke, and Christof Sommitsch. 2020. "Influence of Melt-Pool Stability in 3D Printing of NdFeB Magnets on Density and Magnetic Properties." *Materials* 13 (1):139.

Sun, Z., X. P. Tan, M. Descoins, D. Mangelinck, S. B. Tor, and C. S. Lim. 2019. "Revealing hot tearing mechanism for an additively manufactured high-entropy alloy via selective laser melting." *Scripta Materialia* 168:129-33.

Sun, Zhongji, Xipeng Tan, Shu Beng Tor, and Chee Kai Chua. 2018. "Simultaneously enhanced strength and ductility for 3D-printed stainless steel 316L by selective laser melting." *NPG Asia Materials* 10:127-36.

Sutton, Austin T., Caitlin S. Kriewall, Sreekar Karnati, Ming C. Leu, and Joseph W. Newkirk. 2020. "Characterization of AISI 304L stainless steel powder recycled in the laser powder-bed fusion process." *Additive Manufacturing* 32:100981.

Tan, Joel Heang Kuan, Swee Leong Sing, and Wai Yee Yeong. 2020. "Microstructure modelling for metallic additive manufacturing: a review." *Virtual and Physical Prototyping* 15 (1):87-105.

Tan, Xipeng, Yihong Kok, Yu Jun Tan, Marion Descoins, Domnique Mangelinck, Shu Beng Tor, Kah Fai Leong, and Chee Kai Chua. 2015. "Graded microstructure and mechanical properties of additive manufactured Ti–6Al–4V via electron beam melting." *Acta Materialia* 97:1-16.

Tian, Jian, Wenzhi Zhu, Qingsong Wei, Shifeng Wen, Shuai Li, Bo Song, and Yusheng Shi. 2019. "Process optimization, microstructures and mechanical properties of a Cu-based shape memory alloy fabricated by selective laser melting." *Journal of Alloys and Compounds* 785:754-64.

Tsai, Chun-Yu, Chung-Wei Cheng, An-Chen Lee, and Mi-Ching Tsai. 2019. "Synchronized multi-spot scanning strategies for the laser powder bed fusion process." *Additive Manufacturing* 27:1-7.

Wan, H. Y., Z. J. Zhou, C. P. Li, G. F. Chen, and G. P. Zhang. 2019. "Effect of scanning strategy on mechanical properties of selective laser melted Inconel 718." *Materials Science and Engineering: A* 753:42-8.

Wang, C., X. P. Tan, Z. Du, S. Chandra, Z. Sun, C. W. J. Lim, S. B. Tor, C. S. Lim, and C. H. Wong. 2019. "Additive manufacturing of NiTi shape memory alloys using pre-mixed powders." *Journal of Materials Processing Technology* 271:152-61.

Wang, Di, Guangzhao Ye, Wenhao Dou, Mingkang Zhang, Yongqiang Yang, Shuzhen Mai, and Yang Liu. 2020. "Influence of spatter particles contamination on densification behavior and tensile properties of CoCrW manufactured by selective laser melting." *Optics & Laser Technology* 121:105678.

Wang, J. C., Y. J. Liu, P. Qin, S. X. Liang, T. B. Sercombe, and L. C. Zhang. 2019. "Selective laser melting of Ti–35Nb composite from elemental powder mixture: Microstructure,

mechanical behavior and corrosion behavior." *Materials Science and Engineering: A* 760:214-24.

Wang, Jingjing, Wen Jin Wu, Wei Jing, Xipeng Tan, Gui Jun Bi, Shu Beng Tor, Kah Fai Leong, Chee Kai Chua, and Erjia Liu. 2019. "Improvement of densification and microstructure of ASTM A131 EH36 steel samples additively manufactured via selective laser melting with varying laser scanning speed and hatch spacing." *Materials Science and Engineering: A* 746:300-13.

Wang, Y. C., L. M. Lei, L. Shi, H. Y. Wan, F. Liang, and G. P. Zhang. 2020. "Scanning strategy dependent tensile properties of selective laser melted GH4169." *Materials Science and Engineering: A* 788:139616.

Wen, Shifeng, Chong Wang, Yan Zhou, Longchen Duan, Qingsong Wei, Shoufeng Yang, and Yusheng Shi. 2019. "High-density tungsten fabricated by selective laser melting: Densification, microstructure, mechanical and thermal performance." *Optics & Laser Technology* 116:128-38.

Wong, H., K. Dawson, G. A. Ravi, L. Howlett, R. O. Jones, and C. J. Sutcliffe. 2019. "Multi-Laser Powder Bed Fusion Benchmarking—Initial Trials with Inconel 625." *The International Journal of Advanced Manufacturing Technology* 105:2891-906.

Xiong, Zhengang, Panpan Zhang, Chaolin Tan, Dongdong Dong, Wenyou Ma, and Kun Yu. 2020. "Selective Laser Melting and Remelting of Pure Tungsten." *Advanced Engineering Materials* 22:1901352.

Xiong, Zhiwei, Zhonghan Li, Zhen Sun, Shijie Hao, Ying Yang, Meng Li, Changhui Song, Ping Qiu, and Lishan Cui. 2019. "Selective laser melting of NiTi alloy with superior tensile

property and shape memory effect." *Journal of Materials Science & Technology* 35 (10):2238-42.

Yang, C., Y. J. Zhao, L. M. Kang, D. D. Li, W. W. Zhang, and L. C. Zhang. 2018. "High-strength silicon brass manufactured by selective laser melting." *Materials Letters* 210:169-72. doi: 10.1016/j.matlet.2017.09.011.

Yang, Jingjing, Hanchen Yu, Jie Yin, Ming Gao, Zemin Wang, and Xiaoyan Zeng. 2016. "Formation and control of martensite in Ti-6Al-4V alloy produced by selective laser melting." *Materials & Design* 108:308-18. doi: 10.1016/j.matdes.2016.06.117.

Yap, C. Y., C. K. Chua, Z. L. Dong, Z. H. Liu, D. Q. Zhang, L. E. Loh, and S. L. Sing. 2015. "Review of selective laser melting: Materials and applications." *Applied Physics Reviews* 2 (4):041101.

Yu, W. H., S. L. Sing, C. K. Chua, C. N. Kuo, and X. L. Tian. 2019. "Particle-Reinforced Metal Matrix Nanocomposites Fabricated by Selective Laser Melting: A State of the Art Review." *Progress in Materials Science* 104:330-79.

Yu, Wenhui, Swee Leong Sing, Chee Kai Chua, and Xuelei Tian. 2019. "Influence of re-melting on surface roughness and porosity of AlSi10Mg parts fabricated by selective laser melting." *Journal of Alloys and Compounds* 792:574-81.

Zhang, Changchun, Haihong Zhu, Zhiheng Hu, Luo Zhang, and Xiaoyan Zeng. 2019. "A comparative study on single-laser and multi-laser selective laser melting AlSi10Mg: defects, microstructure and mechanical properties." *Materials Science and Engineering: A* 746:416-23.

Zhang, Xaobing, Bo Cheng, and Charles Tuffile. 2020. "Simulation study of the spatter removal process and optimization design of gas flow system in laser powder bed fusion." *Additive Manufacturing* 32:101049.

Zhou, Linrong, Bo Song, Ruidi Li, Qingsong Wei, Chunze Yan, and Yusheng Shi. 2020. "Effect of element evaporation on the microstructure and properties of CuZnAl shape memory alloys prepared by selective laser melting." *Optics & Laser Technology* 127:106164.